Available online at www.sciencedirect.com
ScienceDirect
Spectrochimica Acta Part A 71 (2008) 616–620
SPECTROCHIMICA ACTA PART A
www.elsevier.com/locate/saa

Synthesis and characterization of new nano-particles as blue ceramic pigment

I.S. Ahmed*, H.A. Dessouki, A.A. Ali

Chemistry Department, Faculty of Science, Benha University, Benha City, Egypt

Received 28 August 2007; accepted 18 December 2007

Abstract

The synthesis of a new nano-blue ceramic pigment $Co_xMg_{1-x}Al_2O_4$ ($0 \leq x \leq 0.1$) using the combination between co-precipitation and combustion synthesis (CS) method. The structure of pigments is assigned based on thermogravimetric and differential thermogravimetric analysis (TG-DTGA), X-ray diffractions (XRD), and UV–vis spectroscopy. Also, diffuse reflectance spectroscopy (DRS) using CIE $L^*a^*b^*$ parameter measurement method, infrared spectroscopy (IR) and transmission electron microscopy (TEM) is used. The result revealed that the nano-size particle pigment was obtained in range 24–35 nm by using 3-methyl-pyrozole-5-one (3MP5O) as a fuel at 400 °C in open furnace. Also, results show the varying colors and particles' size as a result of different calcination temperatures from 500 to 1200 °C for 2 h.

Keywords: Ceramic pigment; X-ray analysis; TGA/DTA; Diffuse reflectance spectroscopy (DRS)

1. Introduction

Inorganic pigments used in plastic, polymer, paints, glasses and ceramics have traditionally been based on transition metal compounds [1]. Modification of physical properties of solid solution can be associated with dopants cations and with changes defect in crystal structure [2]. The Co_2SiO_4 olivine, $(Co, Zn)_2SiO_4$ willemite, $CoAl_2O_4$ spinel, Co_2SnO_4, $(Co, Zn)Al_2O_4$, $Co(Al, Cr)_3O_4$ and $(Co, Zn)TiO_3$ are further blue pigments [3]. The traditional source of blue in ceramic pigment depends on cobalt ion. The color performance of cobalt pigment depends very much on their thermal stability, chemical reactivity towards the glaze components and also on the coordination of Co^{2+} ions (tetrahedral coordination is preferred to octahedral) [4]. Ceramic pigment synthesized by several solution techniques such as sol–gel [5], emulsion precipitation [6], hydrothermal [7], Penchini method [8,9], low combustion method [10–13]. The synthesis routs are very important for determining the final properties of inorganic pigment as color, particle size, resistance to acids and alkaline. In this study, the nano-particles of $Co_xMg_{1-x}Al_2O_4$ spinel pigment prepared by the combination of co-precipitation and combustion method (CS) at low temperature.

2. Experimental

2.1. Materials and reagent

In particular, the starting chemicals used in this study are: aluminum chloride hexahydrate ($AlCl_3{\cdot}6H_2O$), magnesium chloride hexahydrate ($MgCl_2{\cdot}6H_2O$) and cobalt chloride hexahydrate ($CoCl_2{\cdot}6H_2O$), urea (H_2NCONH_2) (Aldrich), sodium carbonate (Merck), nitric acid 65% (Merck), ethylacetoacetate (Aldrich) and hydrazine hydrate (99.9%) (Merck).

2.2. Synthesis of 3-methyl-pyrazole-5-one (3MP5O)

3MP5O ($C_4H_6N_2O$) was prepared by the dropwise addition of 1 mol ethylacetoacetate to 1 mol of hydrazine hydrate (99.9%) cooled in an ice bath according to the following equation:

$$CH_3COCH_2COOC_2H_5 \Downarrow\leftarrow N_2H_4{\cdot}H_2O$$
$$\rightarrow\leftarrow C_4H_6N_2O \Downarrow\leftarrow H_2O \Downarrow\leftarrow C_2H_5OH$$

2.3. Preparation of ceramic pigment

The mixture of calculated stoichiometric amounts of metal salts (aluminum chloride, magnesium chloride and cobalt chloride) was dissolved in distilled water, co-precipitated by using sodium carbonate, thoroughly washed by hot distilled water and dried. This mixture was dissolved in small amount of nitric acid

---

* Corresponding author.
E-mail address: isahmed61@yahoo.com (I.S. Ahmed).

1386-1425/$ – see front matter © 2008 Published by Elsevier B.V.
doi:10.1016/j.saa.2007.12.050

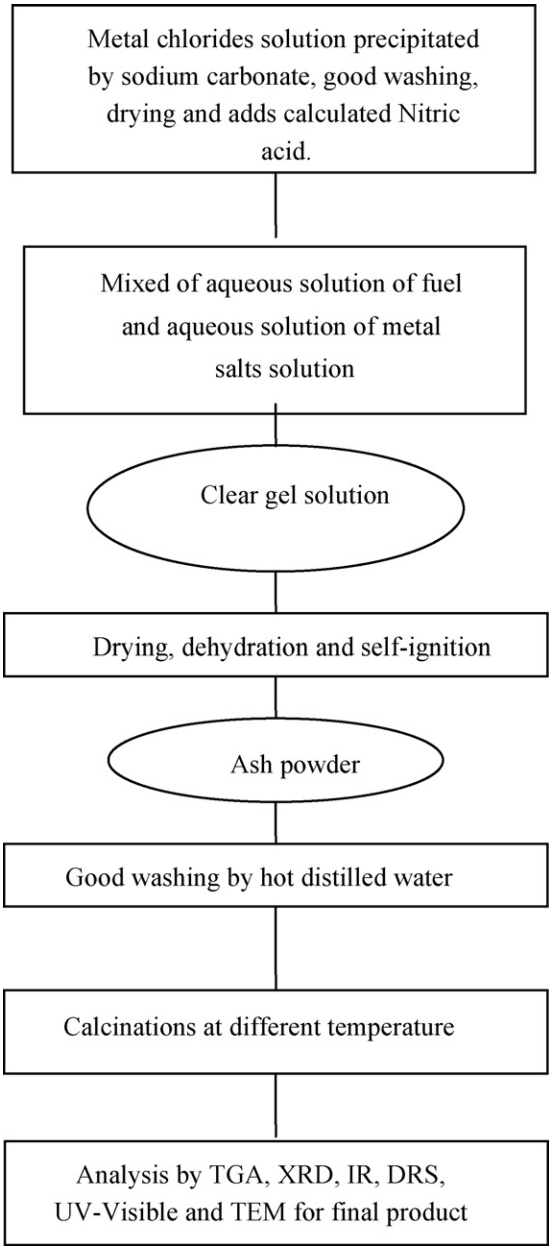

Fig. 1. The flow chart of preparation of pigment powder and analysis methods.

on hot plate to become a clear solution and then cooled using ice. The mixture salts producing mixed with fuel (3MP5O) that is dissolved in small amount of distilled water in Pyrex glass vessel. The resulting solution was heated on a hot plate until a clear gel solution with a small amount of water was transferred into a muffle furnace that was preheated to 400–500 °C. This solution boils, froths, dehydrates and spontaneously ignited exothermic reaction by burning of the metal nitrates and fuel with the release of N_2, CO_2 and H_2O gases. The combustion reaction was completed within a few minutes, and the ash voluminous and fluffy in nature or colored powder was obtained from some of the redox reaction systems of fuel-nitrate dependent on the type of the fuels. The flow chart of the process is shown in Fig. 1.

2.4. Instruments

Thermogravimetric analysis (TGA; TA Instruments, SDT2960) of the precursor was carried out at a heating rate of 10 °C/min in static air. Phase formation of product was identified by using X-ray diffraction (XRD; SIEMENS D5000) with Cu Kα radiation. Transmission electron microscopy (TEM, modal EM 10 Zeiss, at 60 kV) was used to study the morphology of the synthesized powders by dispersing in water on a copper grid. The functional groups characterized by infrared (IR) spectroscopy in 400–4000 range for the calcination powders at different temperatures by using Jasco FT/IR-460 plus by employing potassium bromide KBr, pellet technique. The diffuse reflectance of fired pigments was measured in Jasco spectrophotometer UV–vis in 300–800 nm range using standard D65 illumination and barium sulfate as a reference. The CIE $L^*a^*b^*$ colorimetric method, recommended by the Commission Internationale de l'Eclairage (CIE) [14] was followed. In this method, L^* is lightness axis: black (0) – white (100), b^* is the blue (−) – yellow (+), a^* is the green (−) – red (+) axis and ΔE is the hue variation $\Delta E^2 = (L^*)^2 + (a^*)^2 + (b^*)^2$.

3. Results and discussion

In general, a good fuel used in a combustion process should react non-violently, produce non-toxic gases, and act as a complexing agent for metal cations [15]. For different metal cations, various organic fuels with different ligand groups, i.e. carboxylic group and/or amine group may exhibit different complex power. This is one of the important factors that affect the phase formation and morphology of the final product. In addition, the chemical energy released from the exothermic reaction between various metal nitrates and various fuels is different. This is another important factor that affects the phase formation of the final product because high temperature is in favor of the stable phase formation and particle aggregation of the final product.

Thermal analysis has been carried out on precursor, from TG-curve, the weight losses were calculated for the different steps and compared with those theoretically calculated for the suggested decomposition based on the results of the elemental analysis. TG-curve Fig. 2, shows that the weight loss percentages were 4.9% and 3.5% (calc. 7.9%) at 90–120 °C, this can be attributed to elimination of the water in sample. The weight loss of 23%, at the temperature 200–250 °C, represents the removal of the ligand molecule. The masses remaining at 650 °C were 22.5% corresponding to the removal of CO, CO_2, and NO_x gases from the sample then the solid solution of cobalt aluminate and magnesium aluminate began to be formed at 650 °C. Pyrazolone system is one of the commonly used fuels in low combustion synthesis that contains aliphatic amine and carbonyl groups in their structure.

Infrared (IR) spectra of (0.05%) doping cobalt are present in Fig. 3. From this figure this can be explained that the samples at ignition temperature (500 °C) contain a broad absorption band around 3450 cm^{-1} related to the stretching vibration of free (–OH) group of water. The absorption bands at 1778 and 1100 cm^{-1} are related to the stretching vibration of carbonyl

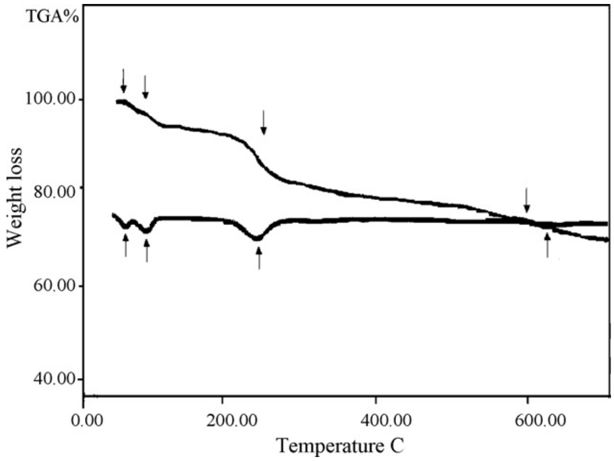

Fig. 2. Thermal analysis of $F = 0.05\%$ Co using (3MP5O) as a fuel.

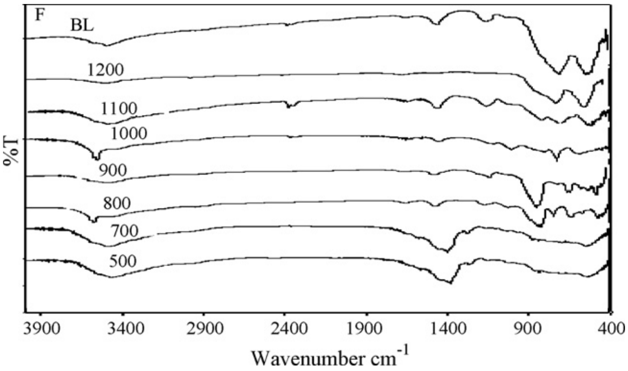

Fig. 3. Infrared spectra for $F = 0.05\%$ Co by using 3MP5O as a fuel.

(C=O, C–O) groups of residual organic fuel. The absorption bands at 1658, 1383 and 825 cm^{-1} correspond to undecomposed nitrate ions [16]. Weak absorption bands in the region 400–700 cm^{-1} appear for the formation trace amounts of metal oxides. After calcination at different temperatures from 500 to 1200 °C, the observed absorption bands in the region 800–4000 cm^{-1} are decreased gradually until disappeared at 1100 °C except, the strong absorption band at 3450 cm^{-1} related to the stretching vibration of constitutional water [17,18]. Infrared (IR) data will agree with data of X-ray for formation of the phase under study around 800 °C. The appearance of strong absorption bands lower than 800 cm^{-1} corresponds to metal oxides. Two absorption bands at high frequency (688–531 cm^{-1}) are corresponding to AlO_6 groups building up the magnesium spinel as a result of vibration of ions of valence Al^{3+} in octahedral positions [17] and two other bands at low frequency (520–450 cm^{-1}) are corresponding to CoO_6/Co_4 and MgO_6/MgO_4 groups for the cobalt and magnesium spinel as a result of vibration in the octahedral sites or to mixed vibration of them in octahedral and tetrahedral [19,20] sites.

The X-ray diffraction for calcinated powders at different firing temperatures is shown in Fig. 4. Up to 800 °C, the powders remained X-ray amorphous or contained only small crystallites that were indicated by the broadening lines will agree with data of thermal analysis for the formation of the stable phase. At 900 °C the calcinated powders begin to appear as the spinel of crystalline form producing from amorphous phase. By increasing temperature above 900 °C, intensities of peaks increase gradually until sharpened peaks are observed [21] at 1100 °C and 1200 °C. The crystalline spinel phase content [22] and also the particles' size increase with increasing calcination temperature that is shown in Table 1.

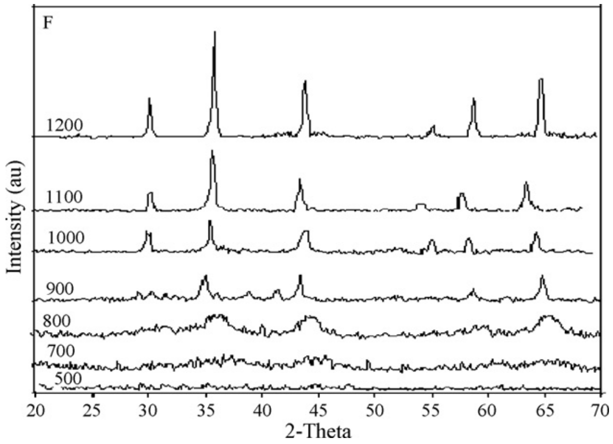

Fig. 4. X-ray diffraction for $A = 0.01$ type at different temperatures using by 3MP5O as a fuel.

Table 1
Particle size from X-ray diffraction for different doping types at different temperatures using 3MP5O as a fuel

Doping	Temperature						
	500	700	800	900	1000	1100	1200
0.01	Am	6.3	7.54	18.89	24.78	30.03	43.28
0.05	Am	4.45	5.98	16.64	21.15	27.25	42.12
0.1	Am	5.77	8.92	15.9	17.1	23.73	30.83

Am: amorphous.

TEM photographs of samples show the spherical particles as present in Fig. 5. The particles' size observed by TEM is in agreement that is observed by XRD as present in Table 2.

UV–vis spectra of doping of cobalt at different calcination temperatures show that three broad absorption bands at 544 (green region), 580 (yellow-orange region) and 630 (red region) nm indicate tetrahedral co-ordination of cobalt [23] which gives rise to the blue coloration as present in Fig. 6. The energy level diagram gives d–d transitions of cobalt Co(II) ($3d^7$) from Orgel diagram shows the present of three transition $^4A_2(F)\cdots{}^4T_2(F)$, $^4A_2(F)\cdots{}^4T_1(F)$ and $^4A_2(F)\cdots{}^4T_1(P)$. The wide and intense absorption band between 500 and 700 nm could be attributed

Table 2
XRD crystallite and TEM particle size different doping types at 1100 °C using 3MP5O as a fuel

%Co	Particle size (nm)	
	X-ray	TEM
0.01	30.03	34.8
0.05	27.25	32.2
0.1	23.73	28.6

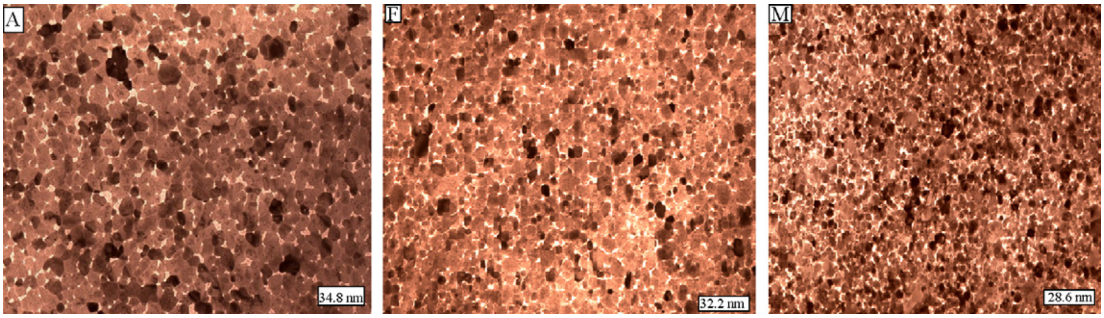

Fig. 5. TEM of $A = 0.01$, $F = 0.05$ and $M = 0.1\%$ Co system at 1100 °C temperature by using 3MP5O as a fuel.

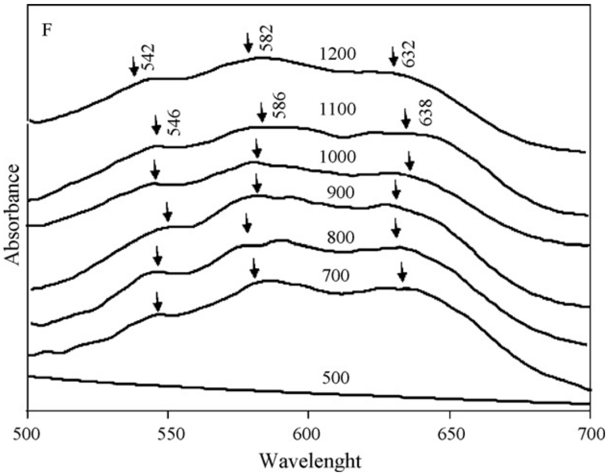

Fig. 6. UV–vis spectra of 0.05% doping of cobalt at different calcination temperatures.

to third transition from $^4A_2(F)(e^4t_2^3)$ as ground state to the excited $^4T_1(P)(e^3t_2^4)$ state. This triple band in visible region can be attributed to Jahn–Teller distortion of tetrahedral structure [24–26].

Diffuse reflectance spectroscopy (DRS) indicates the appearance of band 500 cm^{-1} at 700 °C that tends to pale blue color of sample and this band shifts to the left as calcinated temperatures increase until reaching 480 cm^{-1} at 1000 °C for blue color and 450 cm^{-1} at 1100 °C shows the bluest color pigment [27] as present in Fig. 7.The starting of color appearance from diffuse reflectance data agrees with thermal analysis and X-ray diffraction data around 700 °C. Diffuse reflectance data are presented in Table 3 and show that the values of a^* are random while L^* values decrease and b^* values increase in negative direction as a result of increasing calcination temperatures. We believe that doping is due to the presence of higher amount of defects in structure. These defects lead to the distorted tetrahedral and octahedral sites in spinel structure, changing the ligand-field around the chromophore and hence changing the observed color [8]. The values of b^* are increasing in negative direction, the higher the intensity of blue color. The decreasing L^* parameter tends to reduce the lightness of sample. At the same time, with the increase in the amount of Cobalt percent, the value of b^* increases as present in Fig. 8, leading to the depth of blue color as result of calcination temperatures. The lower value of hue variation ΔE tends to a good color matching [28]. Diffuse reflectance data show the high value of b^* at 1100 °C and lower value of hue variation ΔE at 1200 °C for all doping cobalt percents. This means that the appearance of good pigment powder color occurs at 1100 °C and a good color matching at 1200 °C.

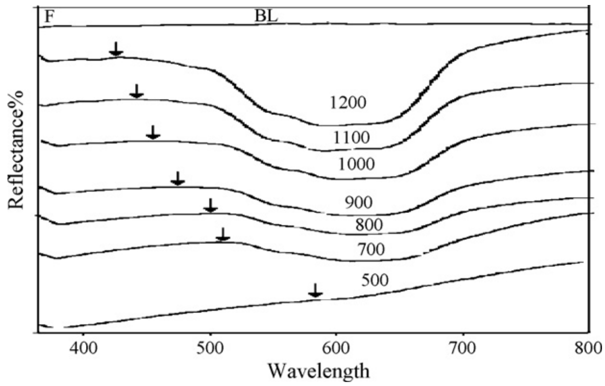

Fig. 7. Diffuse reflectance of $F = 0.05\%$ Co system at different calcinations temperature by using 3MP5O as a fuel.

Table 3
Colorimetric data for A, F and M systems by using 3MP5O as a fuel

System	Temperature	L^*	a^*	b^*	ΔE
0.01	500	95.58	0.60	4.01	95.67
	700	95.09	−0.84	−0.31	95.09
	800	96.64	−1.49	−2.92	96.69
	900	95.77	−1.30	−2.96	95.83
	1000	95.50	−1.85	−4.42	95.62
	1100	95.02	−2.35	−6.17	95.18
	1200	93.04	−1.86	−5.05	93.26
0.05	500	94.70	1.18	4.41	94.81
	700	93.29	−3.08	0.70	93.34
	800	95.19	−2.48	−1.22	95.23
	900	93.65	−2.71	−4.16	93.78
	1000	92.69	−2.18	−6.34	92.93
	1100	92.00	−2.56	−10.72	92.66
	1200	91.77	−1.72	−8.17	92.15
0.1	500	94.11	1.02	4.79	91.9
	700	93.06	−2.79	−2.33	92.34
	800	95.39	−2.41	−3.32	94.94
	900	95.24	−2.57	−5.73	93.36
	1000	94.87	−2.52	−8.07	92.4
	1100	93.26	−4.01	−16.84	87.44
	1200	92.29	−2.82	16.56	86.1

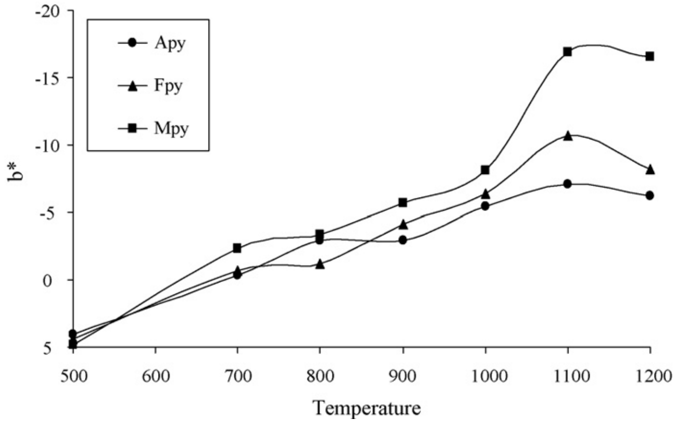

Fig. 8. Color coordinates (b^*) variation with calcinations temperature for $A = 0.01$, $F = 0.05$ and $M = 0.1$ systems.

4. Conclusions

Blue ceramic pigment $Co_xMg_{1-x}Al_2O_4$ is produced as a solid solution from two mixed phases $CoAl_2O_4$ and $MgAl_2O_4$ spinels. This powder prepared by combustion synthesis method (CS) using 3-methyl-pyrozole-5-one (3MP5O) as a fuel at 400 °C in open furnace. Powders are crystallized after calcination at different temperatures and characterized by different tools. The particle size of powder was produced in range 24–35 nm that indicates for the present of nano-size particles. Different degrees of blue color were produced at different calcination temperatures. The bluest color was produced at 1100 °C and a very good matching at 1200 °C from colorimetric data.

References

[1] F. Fernandez, C. Colon, A. Duran, R. Barajas, A. d'Ors, M. Becerril, J. Llopis, S.E. Paje, R. Saez-Puche, I. Julian, The Y_2BaCuO_5 oxide as green pigment in ceramics, J. Alloys Compd. 277 (1998) 750.

[2] M. Karazawa, E. Tomaszewice, Diffuse reflectance spectra of iron vandates, Spectrochim. Acta Part A 55 (1999) 2889.

[3] R.K. Mason, Use of cobalt colors in glazes, J. Am. Ceram. Soc. Bull. 40 (1961) 5.

[4] G. Monari, T. Manfredini, Coloring effects of synthetic inorganic cobalt pigments in fast-fired porcelainized tiles, J. Ceram. Eng. Sci. Process. 17 (1996) 102.

[5] D. Segal, Chemical synthesis of ceramic materials, J. Mater. Chem. 7 (1997) 1297.

[6] M. lade, H. Mays, J. Schmidt, R. Willumeit, R. Schomacker, On the nanoparticle synthesis in microemulsions: detailed characterization of an applied reaction mixture, Colloids Surfaces A, Physchem. 163 (2000) 3.

[7] R.E. Riman, W.L. Suchanek, M.M. Lencka, Hydrothermal crystallization of ceramics, J. Ann. Chim. -Sci. Mat. 27 (2002) 15.

[8] J.D. Cunha, D.M.A. Melo, A.E. Martinelli, M.A.F. Melo, I. Maia, S.D. Cunha, Ceramic pigment obtained by polymeric precursors, Dyes Pigments 65 (2005) 11.

[9] W. Seok Cho, M. Kakihana, Crystallization of ceramic pigment $CoAl_2O_4$ nanocrystals from Co–Al metal organic precursor, J. Alloys Compd. 287 (1999) 87.

[10] C.C. Hwang, T.Wu. Yung, J. Wan, J.S. Tsai, Development of a novel combustion synthesis method for synthesizing of ceramic oxide powders, J. Mater. Sci. Eng. B 111 (2004) 49.

[11] S.T. Aruna, S. Ghosh, K.C. Patil, Combustion synthesis and properties of $Ce_{1-x}Pr_xO_{2-\delta}$ red ceramic Pigments, Int. J. Inorg. Mater. 3 (2001) 387.

[12] K. Du, H. Zhang, Preparation and performance of spinel $LiMn_2O_4$ by a citrate route with combustion, J. Alloys Compd. 352 (2003) 250.

[13] S. Ekambaram, Combustion synthesis and characterization of new class of ZnO-based ceramic pigments, J. Alloys Compd. 390 (2005) 14.

[14] CIE, Recommendations of Uniform Color Spaces, Color Difference Equations, Psychometrics Color Terms, Supplement no. 2 of CIE Publ. No. 15 (E1-1.31), 1971, Bureau Central de la CIE, Paris, 1978.

[15] V.C. Sousa, A.M. Segadaes, M.R. Morelli, R.H.G.A. Kimina, Combustion synthesized ZnO powders for varistor ceramics, Int. J. Inorg. Mater. 1 (1999) 235.

[16] P. Duran, J. Tartaj, F. Rubio, C. Moure, O. Pena, Synthesis and sintering behavior of spinel-type $Co_xNiMn_{2-x}O_4$ prepared by the ethylene glycol-metal nitrate polymerized complex process, J. Ceram. Int. 31 (2005) 599.

[17] M.F.M. Zawrah, A.A. El Kheshen, Synthesis and characterization of nanocrysalline $MgAl_2O_4$, Br. Ceram. Trans. 101 (2002) 71.

[18] A.K. Adak, A. Pathak, A. Pramanik, Polyvinyl alcohol evaporation method for preparation of submicron chromite powders, Br. Ceram. Trans. 98 (1999) 200.

[19] A.Yu. Chapskaya, N.I. Radishevskaya, N.G. Kasatskii, O.K. Lepakova, Yu.S. Naiborodenko, V.V. Vereshchagin, The effect of composition and synthesis conditions on the structure of cobalt bearing pigment of the spinel types, J. Glass Ceram. 62 (2005) 11.

[20] L.F. Koroleva Chekhomova, Synthesis of spinel-based ceramic pigments from hydrocarbonates, Glass Ceram. 61 (2004) 9.

[21] P. Barpanda, S.K. Behera, P.K. Gupta, S.K. Pratihar, S. Bhattacharya, Chemically induced order disorder transition in magnesium aluminium spinel, J. Eur. Ceram. Soc. 26 (2006) 2603.

[22] D.M.A. Melo, J.D. Cunhaa, J.D.G. Fernandes, M.I. Bernardi, M.A.F. Melo, A.E. Martinelli, Evaluation of $CoAl_2O_4$ as ceramic pigments, Mater. Res. Bull. 38 (2003) 1559.

[23] S. Cavaa, S.M. Tebcherani, S.A. Pianaro, C.A. Paskocimas, E. Longo, J.A. Varela, Structural and spectroscopic analysis of γ-Al_2O_3 to α-Al_2O_3-$CoAl_2O_4$ phase transition, Mater. Chem. Phys. 97 (2006) 102.

[24] T. Mimani, S. Ghosh, Combustion synthesis of cobalt pigment: blue and pink, Curr. Sci. 78 (2000) 892.

[25] C.R. Bambord, The application of the ligand field theory to colored glasses, Phys. Chem. Glasses 3 (1962) 189.

[26] T. Bates, Ligand field theory and absorption spectra of transition-metal ions in glasses, in: Modern Aspects of the Vitreous State, vol. 2, Butterworths, London, 1961, pp. 195–254.

[27] M. Llusar, A. Fores, J.A. Badenes, J. Calbo, M.A. Tena, G. Monros, Color analysis of some cobalt-based blue pigments, J. Eur. Ceram. Soc. 21 (2001) 1121.

[28] F. Bondioli, T. Manfredini, M. Romagnoli, Color matching algorithms in ceramic tile production, J. Eur. Ceram. Soc. 26 (2006) 311.